CoN_4 active sites in a graphene matrix for the highly efficient electrocatalysis of CO_2 reduction

ZHANG Hui-nian*, WANG Hui-qi, JIA Su-ping, CHANG Qing, LI Ning, LI Ying, SHI Xiao-lin, LI Zi-yuan, HU Sheng-liang*

（*School of Energy and Power Engineering*, *North University of China*, *Taiyuan* 030051, *China*）

Abstract: Developing highly selective, economical and stable catalysts for the electrochemical conversion of CO_2 into value-added carbon products to mitigate both CO_2 emission and the energy crisis is challenging. We report an efficient and robust electrocatalyst for the CO_2 reduction reaction (CO_2RR) by embedding CoN_4 active sites in a graphene matrix. These highly dispersed CoN_4 sites show an extraordinary CO_2RR activity, with a high CO Faradaic efficiency of nearly 95% at −0.76 V (vs. RHE) and remarkable durability. The corresponding overpotential is 0.65 V. Our finding could pave the way for the design at the atomic scale of highly efficient electrocatalysts for the CO_2RR.

Key words: CO_2 electroreduction; Cobalt; Single-atom catalysts; Electrochemistry; Graphene

1 Introduction

Direct aqueous electroreduction of CO_2 into valuable chemicals and fuels powered by electricity from renewable energy is a desirable technology to realize environmental and energy sustainability[1–4]. However, this desired technique faces highly challenging in practical implementation due to the chemical inertness of CO_2 and multiple distribution of products. Moreover, inevitable competition hydrogen evolution reaction (HER) can concomitantly occur with CO_2 reduction in aqueous media[5]. Converting CO_2 into CO by electrolyzing is currently one of the most practical targets owing to the kinetical favor of CO production compared with other CO_2 reduction products[6,7]. Moreover, CO is the key intermediate for the formation of oxygenates and hydrocarbons. In this regard, robust, economical and efficient CO_2 reduction electrocatalysts with good durability and high activity must be developed to highly favor CO production over the competing HER.

To address these issues, various kinds of noble-metals electrocatalysts, such as Pd[8], Ag[9], Au[10], *etc.*, have been screened for the CO_2-to-CO conversion. However, these catalysts still suffer from the sensitivity to poisoning and high cost, which hinder their practical application. The strategy to mitigate these problems is to develop noble-metal-free electrocatalyst for converting CO_2 to CO. N-doped porous carbon supported single non-noble metal electrocatalyst has been widely explored to convert CO_2 to CO at a high efficient in recent years[11–17]. The special electronic structure and maximized atomic efficiency of these single metal active sites make them can be used as a promising electrocatalyst for CO_2RR. The single-atom Co sites have been successfully introduced to graphene matrix by ball milling of cobalt phthalocyanine (CoPc) and graphene, and the relevant performance of CO_2RR has not been reported due to the high cost[18,19]. In order to scale up CO_2RR process for practical implementation, developing of high-performance and economical electrocatalyst is the cornerstone. However, for the purpose of enhancing the performance for CO_2RR, developing a robust single-atom active electrocatalyst with cost-effective still remains a great challenge.

Herein, we report an effective approach for uniformly dispersed CoN_4 center with Co sites anchored on the matrix of graphene (CoN_4/G) for efficient CO_2RR. In brief, the CoN_4/G composite was prepared

Received date: 2021-01-27; **Revised date:** 2021-04-23

Corresponding author: ZHANG Hui-nian, Lecturer. E-mail: zhanghuinian123@163.com;
HU Sheng-liang, Professor. E-mail: hsliang@yeah.net

Supplementary data associated with this article can be found in the online version.

by high-energy ball milling of graphene nanosheets and cobalt tetrasulfonated phthalocyanine (CoTsPc). The electrocatalytic activity of CO_2RR with cobalt macrocycles was investigated in detail. However, CoTsPc macrocycle molecules are dissolved in aqueous electrolyte as CO_2RR catalyst. It is difficult to make gas diffusion electrodes in aqueous electrolyte and separate and recycle the catalyst. The CoTsPc has a similar structure to CoPc with much cheaper price. The resultant CoN_4/G exhibits high CO Faradaic efficiency of ~95% at −0.76 V (vs. RHE) and the corresponding overpotential of 0.65 V. We expect that our findings will pave an avenue for designing novel single-atom electrocatalysts for efficient CO_2RR.

2 Experimental

2.1 Chemicals and materials

Cobalt tetrasulfonated phthalocyanine (99.5%, Aladdin), $KHCO_3$ (99.7%, Sigma-Aldrich), Nafion solution (5%) and Nafion 117 membrane were supplied by Alfa Aesar. Graphite paper (99.95%) was from Qingdao Huarun Graphite Co. Ltd. Carbon paper was from Toray Industries Inc, Toray TGP-H-060. All reagents were used without further purification.

2.2 Material synthesis

2.2.1 Synthesis of CoN_4/G

The graphene flake (G) was prepared by an electrochemical method[7]. The CoN_4/G synthesis was similar to the previous report[18]. Briefly, 2.8 g of graphene and 1.2 g of CoTsPc was ball milled for 20 h with the stainless steel balls of 120 g and the diameter of 0.9−1.4 cm. After forming CoN_4/G, the residual CoTsPc was washed out with deionized water, and the CoN_4/G was separated by centrifugation.

2.2.2 Synthesis of N/G

100 mg of graphene and 800 mg of melamine were first mixed in 50 mL ethanol and sonication for 90 min. Ethanol was removed by the rotary evaporation. The as-obtained homogeneous solid mixture was dried in vacuum at 80 °C for 12 h. Finally, the N-doped graphene (N/G) was obtained through the carbonization of the mixture at 800 °C for 2 h under flow of Ar. The heating rate was 5 °C min^{-1} and then cooled naturally.

2.3 Characterization

2.3.1 Material characterizations

Scanning transmission electron microscopy (STEM) images were recorded using a JEM ARM200F equipped with a cold field emission gun and double aberration correctors in Institute of Physics Chinese Academy of Sciences in Beijing. Transmission electron microscopy (TEM) measurement was carried out using a JEM-2100F electron microscope. X-ray photoelectron spectroscopy (XPS) were obtained with a Thermo ESCALAB 250 spectrometer. X-ray diffraction (XRD) was recorded using a D8 ADVANCE A25 system configured with the Cu *Kα* 0.154 06 nm radiation. Raman spectra was carried out on a Jobin-Yvon equipped with 532 nm laser line and HR-800 Raman system. UV-Visible spectra were taken on Shimadzu UV-3600 spectrophotometer. SEM images and EDS maps were acquired on JSM-7001F field-emission system. FT-IR spectra were obtained using a Bruke Vertex 70 V FT-IR spectrometer. The Co K-edge absorption spectra (EXAFS) was acquired on the XAFCA beamline at the Singapore Synchrotron Light Source (SSLS), using a Si (111) double crystal monochromator to record data.

2.3.2 Preparation of working electrode

Catalyst inks were prepared by dispersing 10 mg of catalyst in a mixture of 10 μL of Nafion solution (5%) and 1.0 mL of water-ethanol mixture with the volume ratio of 1∶2. All the catalyst inks were sonicated for 1 h to ensure uniform mixing. The working electrode was fabricated by casting a certain amount of catalyst inks onto a 1 × 1 cm^2 porous conductive carbon paper with the loading amount of 2 ± 0.2 mg.

2.3.3 Electrochemical measurements

CO_2RR performance was performed on an electrochemical workstation (CHI760E). The CO_2 reduction reaction occurred in a gas tight H cell configuration, which was separated by Nafion 117 membrane. The carbon paper modified with the catalyst was used as the working electrode of 1 cm^2. A saturated calomel reference electrode (SCE) and a Pt sheet

counter electrode were used. In this work, the SCE electrode was adjusted to the reversible hydrogen electrode (RHE) by the formula: $E_{RHE} = E_{SCE} + 0.24\ V + 0.0591 \times pH$. The CO_2 electrocatalytic conversion was investigated in 30 mL of CO_2 (99.999 9%) saturated with 0.1 mol L^{-1} of $KHCO_3$ solution. The pH of this solution was 6.8. The $KHCO_3$ electrolyte was sparged with CO_2 for 60 min prior to the measurement. The scan rate of linear sweep voltammetry (LSV) is 20 mV s^{-1}. FE are the average values of three GC measurements and the GC measurement repeats every 15 min.

2.3.4 Catalytic product analysis

Gas products were quantified on an online GC equipped with flame ionization detector and thermal conductivity detector. The GC was calibrated using calibration gas, which was commercially available from Dalian Special Gases Co. Ltd.

The liquid products were quantified through an NMR spectroscope with water suppression. After electrolysis, 0.5 mL of $KHCO_3$ electrolyte was mixed with 0.1 mL of D_2O in an NMR tube and dimethyl sulfoxide (DMSO, 0.05 μL) as an internal standard.

The calculation of Faradaic efficiency (FE) for gaseous products using the following equation[15]:

$$FE = \frac{J_{CO}}{J_{total}} = \frac{\upsilon_{CO} \times N \times F}{J_{total}}$$

where, FE is faradaic efficiency for CO production; J_{total} (mA cm^{-2}) is total current density; J_{CO} (mA cm^{-2}) is the partial current density for CO production; v_{CO} is volume concentration of CO (GC data); F is Faradaic constant, F = 96 485 C mol^{-1}; N is the number of electron transferred for product formation.

3 Results and discussion

In this work, atomically dispersed CoN_4 on graphene matrix, denoted as CoN_4/G, was synthesized via high-energy ball milling of graphene nanosheets and CoTsPc for 20 h followed by deionized water washing to remove residual CoTsPc with the highly water solubility (Fig. 1a and Fig. S1b). Furthermore, in Fig. S1b, the blue was not observed for CoN_4/G, in contrast to a mixed G/CoTsPc sample containing the same amount of CoTsPc by hand lapping.

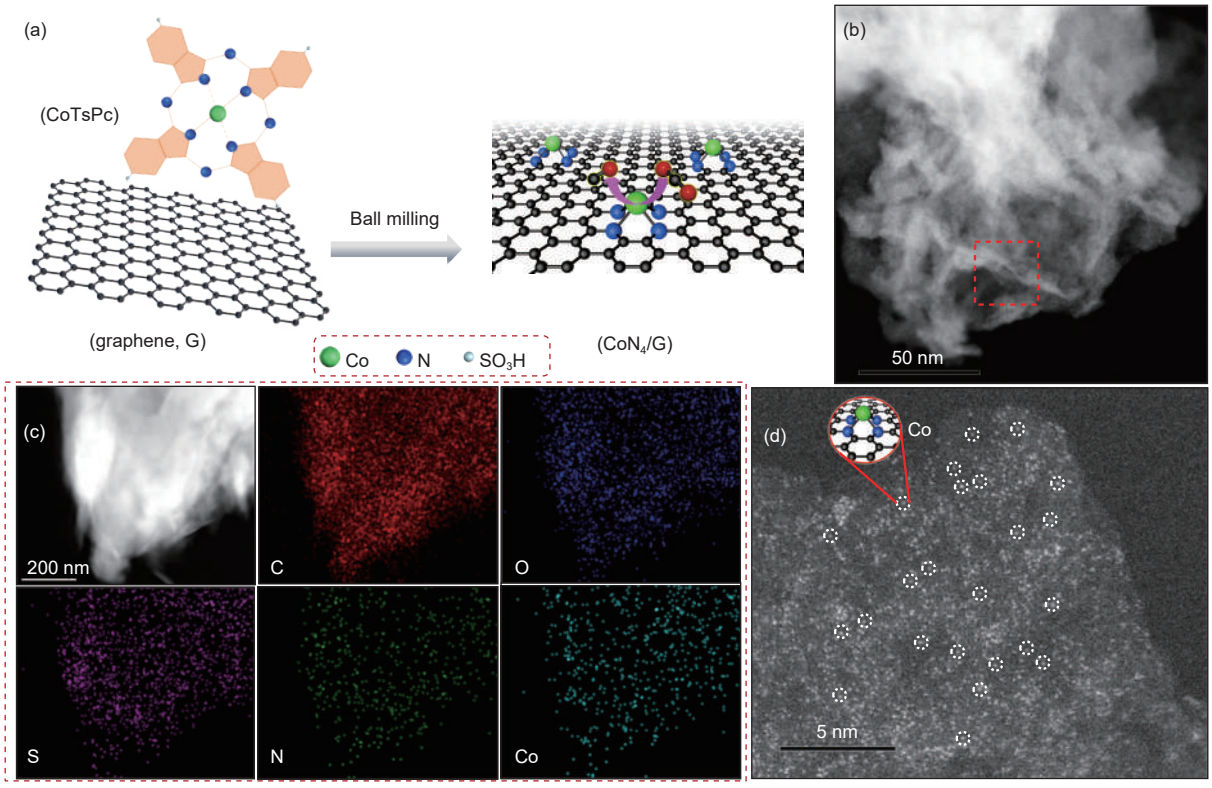

Fig. 1 (a) Illustration of the synthesis route towards CoN_4/G catalyst, (b) STEM image of CoN_4/G, (c) SEM image and the corresponding EDS mapping of CoN_4/G, (d) HAADF-STEM image of CoN_4/G.

This result confirms that the CoTsPc cannot adsorbed on the graphene by mild physical-mixing method. The as-obtained CoN_4/G hybrid material was firstly studied by transmission electron microscopy (TEM), showing the same "sheet-like" structure of graphene (Fig. 1b). The EDS maps of CoN_4/G show that C, N, S and Co are uniform distributed in the graphene network (Fig. 1c). To investigate the atomic structure of Co-N_4 species, the HAADF-STEM imaging was employed. Fig. 1d displays that most bright spots were uniformly dispersed on graphene, which were ascribed to Co atoms.

X-ray absorption near-edge structure (XANES) was employed to further analyze the local coordination structures and chemical environments of Co atoms. As exhibited in Fig. 2a, the Co K edge XANES spectrum for CoTsPc sample showed noticeable spectroscopic signature at approximately 7 716 eV, indicating that CoN_4 in CoTsPc is a planar geometry. By contrast, it was not observed for CoN_4/G catalyst, suggesting its nonplanar structure. When the CoN_4/G catalyst was exposed to air after ball milling, the Co-N_4 sites may be modified by hydroxy groups[18]. Additionally, the fourier-transform (FT) curve shows Co-N coordination structure at about 0.137 nm in CoN_4/G, which is similar to the coordination of Co in the CoTsPc. No other obvious peak for the Co-Co coordination was detected (Fig. 2b)[13,20,21]. According to the XANES spectra, the local CoN_4 structure is well retained. The Raman spectroscopy indicates that the breathing mode (B1g) near 550-1 000 cm^{-1} of the characteristic macrocycle has become very weak in CoN_4/G hybrid catalyst, indicating that the macrocycle structure of CoTsPc may have been destroyed during the ball milling process (Fig. 2c and S5). Furthermore, XRD also confirm the original CoTsPc crystal structure has been destroyed since the characteristic diffraction peaks of CoTsPc in CoN_4/G disappeared (Fig. 2d)[18,19]. The XRD pattern of CoN_4/G presents only two distinct diffraction peaks at approximately 26.15 and 43.31, corresponding well with the (002) and (101) planes of graphitic carbon (Fig. 2d)[22, 23]. The UV-Vis spectra of CoTsPc showed a characteristic absorption peak at approximately 597 nm.

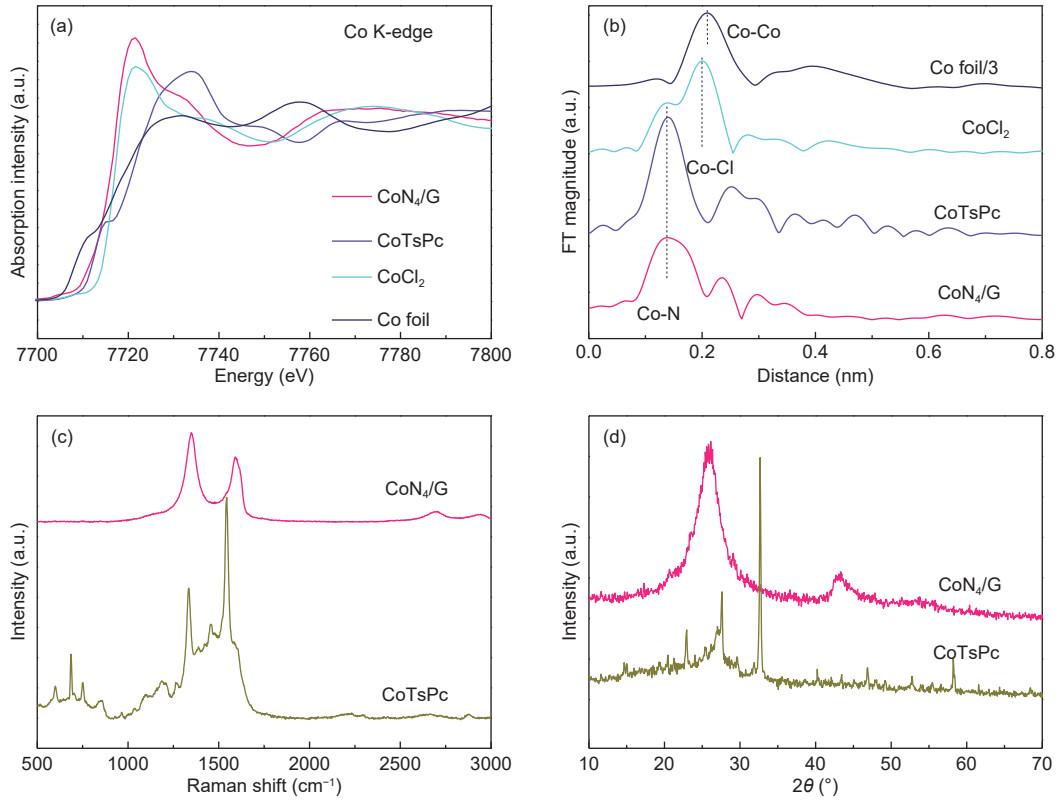

Fig. 2　(a) Co K-edge XANES spectra of CoN_4/G catalyst in comparison with Co foil, $CoCl_2$ and CoTsPc and (b) Fourier transformed (FT) of EXAFS. (c) Raman spectra and (d) XRD patterns of CoN_4/G sample in comparison with CoTsPc.

However, in the case of CoN_4/G catalyst, the absorption peak was disappeared (Fig. S1a), which could be attributed to the reduced aromatic regions caused by the ball milling[24,25]. These characterizations indicated that the crystalline structure of CoTsPc has been destroyed with the residues of CoN_4 species incorporated in graphene through the ball milling[18,19]. The surface atomic compositions of CoN_4/G were acquired by XPS survey spectrum. The survey spectrum indicates the presence of N for 5.36%, C for 63.27%, O for 7.07%, S for 2.64% and Co for 1.66% in CoN_4/G (Fig. 3a and S2). Considering the limited detection depth of XPS test, Co atoms in CoN_4/G were mostly incorporated in carbon layers, the elment contents of CoN_4/G_4 were measured by ICP measurement. The Co content in CoN_4/G was determined to be 1.61%. While the surface C, N, O, S and Co content in CoTsPc is ca. 40.71%, 16.25%, 29.22%, 6.18% and 7.64%, respectively (Fig. S2). The Co 2p spectrum (Fig. 3b) exhibits peaks at 796.5 and 781.3 eV, which matches well with the Co $2p_{1/2}$ orbitals and $2p_{3/2}$ orbitals of a Co^{2+} species, further indicating the valence state of Co-N_4 species was not reduced by ball milling[20,21]. The exhibited two distinct categories of N species including pyrrolic N_α at 401.3 eV combined with Co atom and pyridinic N_β at 399.9 eV bonded with carbon atom of the outer macrocycle (Fig. 3c). The intensity ratio of N_β to N_α in CoN_4/G is significantly reduced compared with CoTsPc. This results indicates that ball milling leads to the destruction of part of the pyridinic N_β species, whereas, pyrrolic N_α species are well maintained in the CoN_4/G sample. Based on the XPS results, we estimated that the Co atoms are embedded in the matrix of graphene and bonded with four pyrrolic N_α atoms, which was consistent with the previous observation for MN_4/GN[18,19]. The S 2p spectrum is shown in Fig. 3d, in which the peaks at 168.5 and 169.1 eV for the sulfate species (SO_X) can be observed in the CoTsPc. While signals from C—S—C groups at 163-165 eV were absent in the CoN_4/G[26,27], indicating that the S atoms were not embedded in graphene lattice after ball milling. The characteristic peak at 1 027 cm^{-1} contributed to the —SO_3H group were absent in the CoN_4/G (Fig. S3)[28].

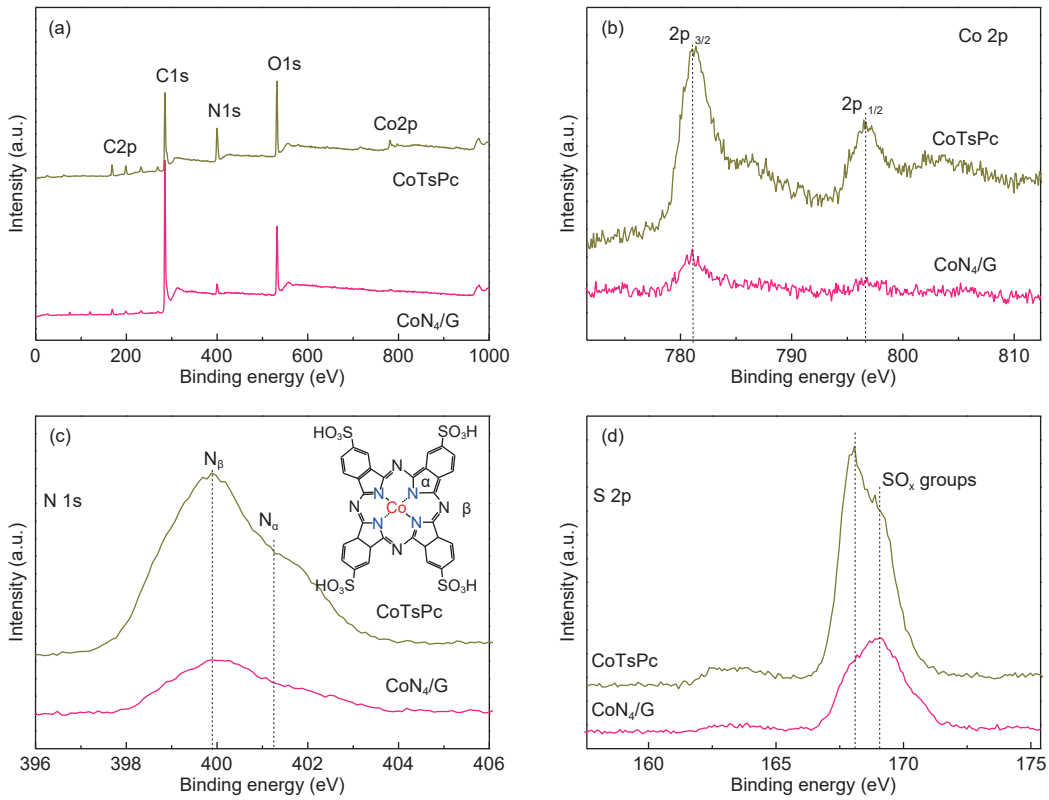

Fig. 3 XPS characterization of CoN_4/G sample in comparison with CoTsPc: (a) XPS full spectra, (b) Co 2p XPS spectra, (c) N 1s XPS (insert of CoTsP structure), and (d) S 2p XPS spectra.

This also clearly indicated the $-SO_3H$ and the outside macrocyclic structure of CoTsPc has been broken during ball milling. According to mechano-chemical process by ball milling, graphitic C—C bonds at the edge in graphene could be homolytic and reacted with $-SO_x-C-$ during ball milling (Fig. S4)[29]. Meanwhile, $-C-SO_x-C-$ groups are predominately located at the edge of the graphene. FT-IR spectrum of CoN_4/G shows a unique sharp peak at 1 562 cm^{-1}, which was associated with S—O stretching exclusively from $-C-SO_x-C-$[28]. Based on the above results, atomically dispersed Co-N_4 species have been successfully embedded in the matrix of graphene through ball milling of CoTsPc and graphene.

The electrocatalytic performance of CO_2 conversion of the CoN_4/G catalyst was evaluated in a two-compartment gas-tight electrochemical cell. The linear sweep voltammetry (LSV) measurements for CoN_4/G catalyst were conducted in Ar- and CO_2- saturated 0.1 mol L^{-1} $KHCO_3$ electrolyte. As shown in CO_2-saturated $KHCO_3$ solution (Fig. 4a), the CoN_4/G catalyst ball milled for 20 h exhibited a low onset potential of −0.41 V (vs. RHE), corresponding 0.30 V in onset overpotential with the standard equilibrium potential of CO_2/CO of −0.11 V at pH 6.8 (vs. RHE)[6]). Meanwhile, the resulting total geometric current density in Ar-saturated solution was far less than those obtained in CO_2-saturated electrolyte. The change in current density alone cannot provide conclusive evidence for CO_2 reduction. This could be ascribed to the interconnevtion of CO_2 reduction and HER. The pH will lower upon CO_2 dissolving in $KHCO_3$, which will in turn further enhance the HER. Thus, the occurrence of CO_2 reduction was further confirmed by analyzing the reduction products.

We employed gas chromatography (GC) to analyze the gaseous products from CO_2RR. Under working potentials between −0.26 and −0.96 V (vs. RHE), CO is observed as the dominant product. No liquid product is detected by ^{1}H NMR spectroscopy in CO_2-saturated electrolyte. While in Ar-saturated electrolyte, no CO is detected. The corresponding FE for CO was measured for CoN_4/G. With the goal of investigating the role of CoN_4 sites in CO_2RR, N/G was prepared (Fig. 4b). N/G was synthesized via pyrolysis the mixture of graphene and melamine. The Raman spectra and XRD pattern of N/G was shown in Fig. S6. The CoN_4/G catalyst presented a higher selectivity for CO formation in comparison with N/G. Specifically, at −0.76 V (vs. RHE) corresponding 0.65 V in overpotential, the CoN_4/G could reach a maximum FE of ~95%, which is comparable to the best single Co atom electrocatalyst reported to date and better than most of the reported N-doped carbon matrix (Fig. S7 and Table S1)[13,20,30–33]. Meanwhile, the FEs of CoN_4/G gradually decreases as the potential changes to more negative value, probably due to the dominant competitive HER[34]. This may indicate that the CoN_4/G catalyst was limited in the mass transport of CO_2 into the single-atom Co sites[35,36]. This observation agrees well with the LSV results. However, the maximum FE of N/G for CO was only 25%. By optimizing the Co content and ball milling time, the CoN_4/G with 1.61% Co ball milled for 20 h was optimized (Fig. S8 and Fig. S10). Fig. 4c showed the CO partial current density (j_{CO}) of CoN_4/G and N/G, which are normalized by the geometrical surface area. The CoN_4/G exhibited a higher j_{CO} than that of N/G at each potential, and the j_{CO} of CoN_4/G reaches up to 19 mA cm^{-2} at −0.96 V, which was 16 times more than that of N/G at the same potential. The CO production rate of CoN_4/G catalyst increased acutely with increased applied potential, and it was significantly superior to N/G catalyst for all the potentials tested (Fig. 4d). The CO_2 reduction activity of CoN_4/G including cobalt element significantly exceeds that of N/G without cobalt, indicating the CoN_4 structure plays a vital role in enhancing CO_2 conversion[20]. Although the N contents of N/G and CoN_4/G are 6.67% and 5.36% respectively (Fig. S2), the as-prepared N/G sample exhibits poor electrochemical activity for CO_2 reduction compared with CoN_4/G catalyst (Fig. 4b-d), excluding the major contribution of nitrogen dopant enhanced the electrocatalytic performance. Thus, the higher catalytic activity of CO_2RR for CoN_4/G was predominately attributed to the CoN_4 doping. The sta-

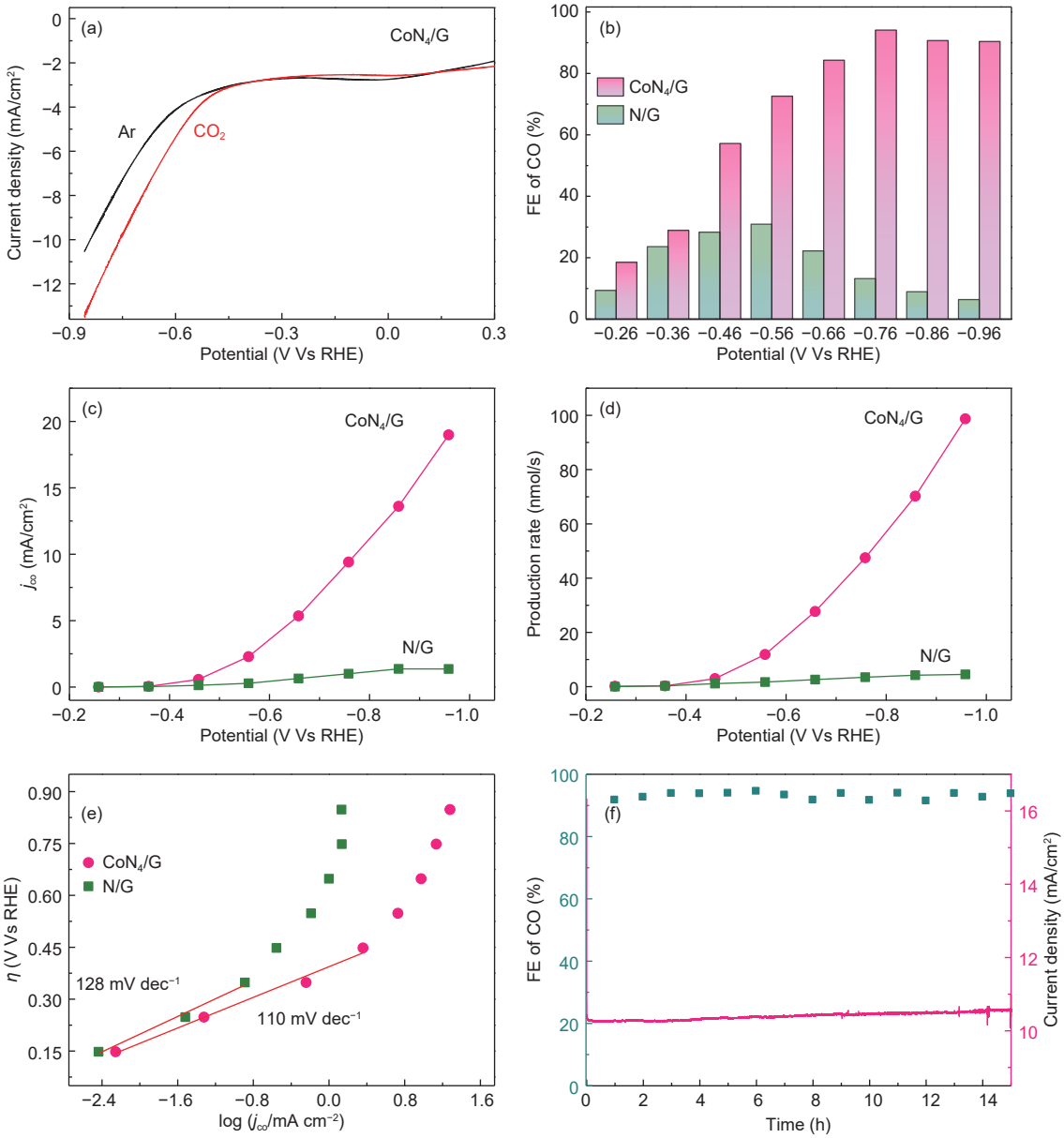

Fig. 4 CO_2RR catalytic performance of as-synthesized catalysts. (a) 20 mV s^{-1} LSV scans for the CoN_4/G catalyst in $KHCO_3$ solution. Comparison of electrocatalytic activity of CoN_4/G and N/G: (b) FE of CO, (c) j_{CO} and (d) production rates of CO at varoius applied potentials. (e) Tafel plot. (f) Long-term stability for CoN_4/G catalyst at −0.76 V (vs. RHE) for 15 h.

bility of CoN_4/G catalyst during long-term operation for CO_2RR was further investigated (Fig. 4f). The current density maintained steadily at ~10.5 mA cm^{-2} and less than 2% decay over 15 h at −0.76 V (vs. RHE). The corresponding FEs of electrochemical CO_2— to —CO conversion maintained constantly (~94%) throughout the test, unambiguously indicating remarkable cycling stability of CoN_4/G catalyst. After the electrolysis of CoN_4/G catalyst, the single Co atoms still remain atomically dispersed on graphene matrix (Fig. S9).

In addition, Tafel analysis was undertaken to further uncover the kinetics of CO_2RR on CoN_4/G catalyst. The Tafel slope of CoN_4/G was 110 mV dec^{-1}, which is smaller than that of N/G with 128 mV dec^{-1}, indicating more favorable kinetics for CO format (Fig. 4e).[13,14]. The Tafel slope of activation process was about 118 mV dec^{-1}[22]. The Tafel slope of CoN_4/G was close to the theoretical value, indicating the similar reaction mechanism. Threfore, the rate-limiting step for CoN_4/G was the initial CO_2 activation process.

4 Conclusion

In conclusion, the atomically dispersed CoN_4 sites have been embedded in the matrix of graphene by a one-step ball milling method, which exhibits an outstanding catalytic performance for CO_2RR. The as-prepared CoN_4/G catalyst affords a high CO FE of about 95% at −0.76 V(vs. RHE), making it comparable to the reported single Co atom electrocatalys. Our results provide a new avenue to design novel SACs for a wide range of electrocatalysis, energy conversion and storage related applications.

Acknowledgement

The authors thank for the financial support from the Scientific and Technological Innovation Programs of Higher Education Institutions in Shanxi (2019L0597, 2019L0557, 2020L0279), the National Natural Science Foundation of China (21703209), the Shanxi Province Science Foundation for Youths (201901D211225), the Talent Introduction Fund of Shanxi Province (18001913), the starting fund for scientific research of North University of China (11012316), the project supported by Science Foundation of North University of China (XJJ201819, XJJ201913) and the Key Research and Development (R&D) Projects of Shanxi Province (201803D121037).

References

[1] Benson E E, Kubiak C P, Sathrum A J, et al. Electrocatalytic and homogeneous approaches to conversion of CO_2 to liquid fuels[J]. Chemical Society Reviews, 2009, 38(1): 89-99.

[2] Chu S, Majumdar A. Opportunities and challenges for a sustainable energy future[J]. Nature, 2012, 488(7411): 294-303.

[3] Zhang L, Zhao Z J, Gong J L. Nanostructured materials for heterogeneous electrocatalytic CO_2 reduction and their related reaction mechanisms[J]. Angewandte Chemie International Edition, 2017, 56(38): 11326-11353.

[4] Zhu D D, Liu J L, Qiao S Z. Recent advances in inorganic heterogeneous electrocatalysts for reduction of carbon dioxide[J]. Advanced Materials, 2016, 28(18): 3423-3452.

[5] Zhang Y J, Sethuraman V, Michalsky R, et al. Competition between CO_2 reduction and H_2 evolution on transition-metal electrocatalysts[J]. ACS Catalysis, 2014, 4(10): 3742-3748.

[6] Zhang C H, Yang S Z, Wu J J, et al. Electrochemical CO_2 reduction with atomic iron-dispersed on nitrogen-doped graphene[J]. Advanced Energy Materials, 2018, 8(19): 1703487.

[7] Zhang H N, Wang J, Zhao Z, et al. The synthesis of atomic Fe embedded in bamboo-CNTs grown on graphene as a superior CO_2 electrocatalyst[J]. Green Chemistry, 2018, 20(15): 3521-3529.

[8] Yuan X T, Zhang L, Li L L, et al. Ultrathin Pd-Au shells with controllable alloying degree on Pd nanocubes toward carbon dioxide reduction[J]. Journal of the American Chemical Society, 2019, 141(12): 4791-4794.

[9] Liu S B, Tao H B, Zeng L, et al. Shape-dependent electrocatalytic reduction of CO_2 to CO on triangular silver nanoplates[J]. Journal of the American Chemical Society, 2017, 139(6): 2160-2163.

[10] Mistry H, Reske R, Zeng Z H, et al. Exceptional size-dependent activity enhancement in the electroreduction of CO_2 over Au nanoparticles[J]. Journal of the American Chemical Society, 2014, 136(47): 16473-16476.

[11] Yang H B, Hung S F, Liu S, et al. Atomically dispersed Ni(I) as the active site for electrochemical CO_2 reduction[J]. Nature Energy, 2018, 3(2): 140-147.

[12] Yang J, Qiu Z Y, Zhao C M, et al. In-situ thermal atomization to transfer supported metal nanoparticles to surface enriched Ni single atom catalyst[J]. Angewandte Chemie International Edition, 2018, 57(43): 14095-14100.

[13] Wang X Q, Chen Z, Zhao X Y, et al. Regulation of coordination number over single Co sites: Triggering the efficient electroreduction of CO_2[J]. Angewandte Chemie International Edition, 2018, 57(7): 1944-1948.

[14] Fan Q, Hou P F, Choi C H, et al. Activation of Ni particles into single Ni-N atoms for efficient electrochemical reduction of CO_2[J]. Advanced Energy Materials, 2019, 10(5): 1903068.

[15] Zhao C M, Dai X Y, Yao T, et al. Ionic exchange of metal-organic frameworks to access single nickel sites for efficient electroreduction of CO_2[J]. Journal of the American Chemical Society, 2017, 139(24): 8078-8081.

[16] Li X G, Bi W T, Chen M L, et al. Exclusive Ni-N_4 sites realize near-unity CO selectivity for electrochemical CO_2 reduction[J]. Journal of the American Chemical Society, 2017, 139(42): 14889-14892.

[17] Zhang Y F, Yu C, Tan X Y, et al. Recent advances in multilevel nickel-nitrogen-carbon catalysts for CO_2 electroreduction to CO[J]. New Carbon Materials, 2021, 36(1): 19-33.

[18] Cui X J, Xiao J P, Wu Y H, et al. A graphene composite material with single cobalt active sites: A highly efficient counter electrode for dye-sensitized solar cells[J]. Angewandte Chemie International Edition, 2016, 55(23): 6708-6712.

[19] Cui X J, Li H B, Wang Y, et al. Room-temperature methane conversion by graphene-confined single iron atoms[J]. Chem, 2018, 4(8): 1902-1910.

[20] Geng Z G, Cao Y J, Chen W X, et al. Regulating the coordination environment of Co single atoms for achieving efficient electrocatalytic activity in CO_2 reduction[J]. Applied Catalysis B: Environmental, 2019, 240: 234-240.

[21] Song X K, Zhang H, Yang Y Q, et al. Bifunctional nitrogen and cobalt co-doped hollow carbon for electrochemical syngas production[J]. Advanced Science, 2018, 5(7): 1800177.

[22] Chen X, Ma D D, Chen B, et al. Metal-organic framework-derived mesoporous carbon nanoframes embedded with atomically dispersed Fe-N_x active sites for efficient bifunctional oxygen and carbon dioxide electroreduction[J]. Applied Catalysis B: Environmental, 2020, 267: 118720.

[23] Luo X Y, Chen Y, Mo Y. A review of charge storage in porous carbon-based supercapacitors[J]. New Carbon Materials, 2021, 36(1): 49-68.

[24] Han N, Wang Y, Ma L, et al. Supported cobalt polyphthalocyanine for high-performance electrocatalytic CO_2 reduction[J]. Chem, 2017, 3(4): 652-664.

[25] Zhu M H, Chen J C, Huang L B, et al. Covalently grafting cobalt porphyrin onto carbon nanotubes for efficient CO_2 electroreduction[J]. Angewandte Chemie International Edition, 2019, 58(20): 6595-6599.

[26] Chen P Z, Zhou T P, Xing L L, et al. Atomically dispersed iron-nitrogen species as electrocatalysts for bifunctional oxygen evolution and reduction reactions[J]. Angewandte Chemie International Edition, 2017, 56(2): 610-614.

[27] Li Q H, Chen W X, Xiao H, et al. Fe isolated single atoms on S, N co-doped carbon by copolymer pyrolysis strategy for highly efficient oxygen reduction reaction[J]. Advanced Materials, 2018, 30(25): 1800588.

[28] Nabid M R, Sedghi R, Jamaat P R, et al. Catalytic oxidative polymerization of aniline by using transition-metal tetrasulfonated phthalocyanine[J]. Applied Catalysis A: General, 2007, 328(1): 52-57.

[29] Jeon I Y, Shin Y R, Sohn G J, et al. Edge-carboxylated graphene nanosheets via ball milling[J]. PNAS, 2012, 109(15): 5588-5593.

[30] Pan Y, Lin R, Chen Y J, et al. Design of single-atom Co-N_5 catalytic site: A robust electrocatalyst for CO_2 reduction with nearly 100% CO selectivity and remarkable stability[J]. Journal of the American Chemical Society, 2018, 140(12): 4218-4221.

[31] Wu J J, Liu M J, Sharma P P, et al. Incorporation of nitrogen defects for efficient reduction of CO_2 via two-electron pathway on three-dimensional graphene foam[J]. Nano Letters, 2016, 16(1): 466-470.

[32] Wu J J, Yadav R M, Liu M J, et al. Achieving highly efficient, selective, and stable CO_2 reduction on nitrogen-doped carbon nanotubes[J]. ACS Nano, 2015, 9(5): 5364-5371.

[33] Xu J Y, Kan Y H, Huang R, et al. Revealing the origin of activity in nitrogen-doped nanocarbons towards electrocatalytic reduction of carbon dioxide[J]. ChemSusChem, 2016, 9(10): 1085-1089.

[34] Jiang K, Siahrostami S, Zheng T T, et al. Isolated Ni single atoms in graphene nanosheets for high-performance CO_2 reduction[J]. Energy & Environmental Science, 2018, 11(4): 893-903.

[35] Zhang H N, Li J, Xi S B, et al. A graphene-supported single-atom FeN_5 catalytic site for efficient electrochemical CO_2 reduction[J]. Angewandte Chemie International Edition, 2019, 58(42): 14871-14876.

[36] Liu Y S, McCrory C C L. Modulating the mechanism of electrocatalytic CO_2 reduction by cobalt phthalocyanine through polymer coordination and encapsulation[J]. Nature Communications, 2019, 10: 1683.